Preprints of the 21st IFAC World Congress (Virtual)
Berlin, Germany, July 12-17, 2020

Analysis of Self-Oscillations in Three-Level Hysteresis Current Controlled H-Bridge

Andreas Krämer * Christian Bohn ** Abid Ali *

* *Technology Transfer Center for E-Mobility, University of Applied Sciences Würzburg-Schweinfurt, 97421 Schweinfurt, Germany (e-mail: andreas.kraemer@ fhws.de, abid.ali@fhws.de).*
** *Institute of Electrical Information Technology, Clausthal University of Technology, 38678 Clausthal-Zellerfeld, Germany (e-mail: christian.bohn@tu-clausthal.de)*

Abstract: In direct-current control scheme, self-oscillations or limit cycles occur due to the hysteresis controller. In this contribution, the different types of self-oscillations in a three-level hysteresis current controlled H-bridge are analyzed. The investigations are based on Tsypkin's method for self-oscillations in relay control systems. So, the conditions for the different types of self-oscillations are given and the frequency of the oscillation and the on-to-off-ratio or pulse width of the switching hysteresis output are calculated exactly. The values correspond to the switching frequency and the duty cycle of the H-bridge. Furthermore, some analyses about the transfer characteristic of the control loop are made.

Keywords: self-oscillation, limit cycle, hysteresis, on-off controller, nonlinear control, stability, electric power system

1. INTRODUCTION

H-bridges or full bridges are used in electrical DC-drives, single-phase AC-drives, single-phase grid injections, etc. In combination with a current regulator, these are able to provide nearly constant or sinusoidal currents with variable frequency and amplitude to the load depending on the application. A common strategy is to use a linear controller, mostly in PI-configuration, in combination with pulse width modulation (PWM). This modulation technique generates the control signals for the H-bridge with an average value proportional to the regulating voltage of the linear controller output, see Holmes and Lipo (2003).

In contrast to a linear controller with PWM, the hysteresis unit directly provides the necessary control signals for the power electronics. These so-called direct-current controllers have some advantages compared to the linear control techniques. In practice, direct-current controllers show good dynamical performance and high robustness against disturbances. The controller keeps the current error bounded in a predefined tolerance.

Irrespective of the controller type, linear or nonlinear, there are two possibilities to drive an H-bridge. One is a two-level control with two different output voltages of the H-bridge, a positive and negative one like in Gatlan and Gatlan (1997). The other is a three-level control with three different output voltages, a positive and a negative one and additional zero voltage, see Mao et al. (2012).

From a control theoretical point of view, the hysteresis control loop has self-oscillations or limit cycles. A theoretical analysis is necessary to categorize these oscillations. In general, self-oscillations in nonlinear control loops can be analyzed by the describing function method, see Atherton (1982) or Gelb and Vander Velde (1968). It linearizes the input/output behavior of the nonlinearity and studies the linearized loop for marginal stability. But this is only an approximation for the occurring self-oscillations. In some cases like in loops with hysteresis controllers and first-order systems, the describing function method provides even no solution although a limit cycle arises, see, for example, Unbehauen (2009) or Gelb and Vander Velde (1968).

Tsypkin (1984) presented an accurate method to determine self-oscillations in relay control systems. Tsypkin's method sums all Fourier harmonics of the hysteresis output or more precisely their transfer to the output of the linear system. As a result, Tsypkin's locus is obtained which is a frequency dependent curve. Similar to the describing function method in combination with Nyquist's locus, the intersections of Tsypkin's locus with the hysteresis limit specify the self-oscillations. Based on Tsypkin's method, Boiko (2009) and Johansson (1997) presented the determination and identification of self-oscillations in two-level hysteresis control system from a state-space description of the linear system. In this paper, Tsypkin's theory is expanded to self-oscillations in three-level hysteresis control loops in general and to hysteresis controlled H-bridge in particular.

The paper is organized as follows. A system overview is given in Section 2. In Section 3, the conditions and the description for the different types of self-oscillations in three-level hysteresis systems are presented. Therefore,

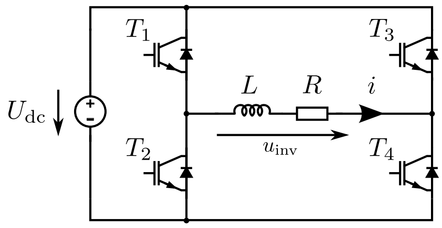

Fig. 1. H-bridge with RL-load

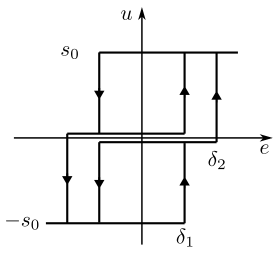

Fig. 2. Three-level hysteresis control element

Tsypkin's loci are set up for these systems with a linear part of any order with additional dead-time. The self-oscillations are also checked for their stability. The general derivations are applied to the H-bridge control system in Section 4, while conclusions are drawn in Section 5.

2. SYSTEM OVERVIEW

The plant consists of an H-bridge or full bridge with four transistors and the connected load. The basic circuit of the plant is shown in Fig. 1. The aim is to control the current i in the RL-load by switching the transistors with the hysteresis controller. So the transfer function from the hysteresis output to the current results in

$$G(s) = \frac{1}{L \cdot s + R} \tag{1}$$

The three level hysteresis controller consist of an upper and a lower subhysteresis unit with symmetrical limits δ_1 and the transitions between these both defined by the hysteresis limit δ_2. So, the whole hysteresis element has a positive, a negative and two zero output stages leading to positive as well as negative load voltage in the H-bridge. The zero stages correspond to two freewheeling circuits. The hysteresis element with its limits and the three output levels is defined by Fig. 2.

For the four different stages or the output of the hysteresis the corresponding transistor conditions are shown in Table 1.

Table 1. Switching table

subhysteresis	u	T_1	T_2	T_3	T_4
upper	$s_0 = U_{\rm dc}$	ON	OFF	OFF	ON
	0	ON	OFF	ON	OFF
lower	0	OFF	ON	OFF	ON
	$-s_0 = -U_{\rm dc}$	OFF	ON	ON	OFF

Caused by a discrete-time implementation of the controller, there is an additional dead-time $T_{\rm t}$ within the control loop as shown in Fig. 3.

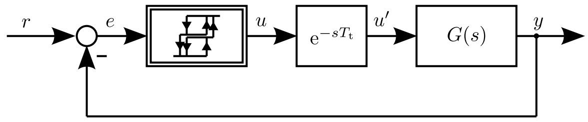

Fig. 3. Three-level hysteresis control loop

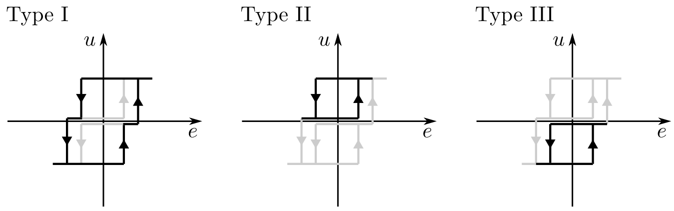

Fig. 4. Different types of oscillation defined by the transition paths of the three-level hysteresis

3. SELF-OSCILLATIONS

In a control loop with a three-level hysteresis element, there are several different types of self-oscillations possible. Their existence or occurrence depends on the linear part of the control loop, the hysteresis limits, the set point as well as the disturbance. Regarding the different transition paths through the three-level hysteresis, three different types of oscillation can be defined. These three types are shown in Fig. 4.

Type I: The path is characterized by all the three output levels of the hysteresis. Starting at the positive level s_0, the path follows the limit $-\delta_1$ to the zero level and further to the level $-s_0$ by the switching limit $-\delta_2$. Afterwards, the way leads back to the positive level s_0 through the limits δ_1 and δ_2 respectively.

Type II: The oscillation only occurs by the upper subhysteresis defined by the two levels s_0 and zero and the symmetrical limits $\pm\delta_1$.

Type III: This type of oscillation is defined by the lower subhysteresis with its two levels zero and $-s_0$ and the symmetrical limits $\pm\delta_1$.

These different types of self-oscillations are studied in the following subsections. The conditions for each one and their stability are established. For this purpose, Tsypkin's loci are derived.

Tsypkin's locus $\mathcal{J}(\omega)$ for a symmetrical self-oscillation in two point hysteresis control loop is defined by

$$\mathcal{J}(\omega) = -\frac{1}{\omega}\dot{\tilde{y}}^{-}\left(\frac{\pi}{\omega}\right) - \mathrm{j}\tilde{y}^{-}\left(\frac{\pi}{\omega}\right) \tag{2}$$

where ω is the frequency. The imaginary part $-\tilde{y}^{-}\left(\frac{\pi}{\omega}\right)$ is the negative output value of the loop at the switching point of the hysteresis in the middle of the period under oscillation with ω. The real part $-\frac{1}{\omega}\dot{\tilde{y}}^{-}\left(\frac{\pi}{\omega}\right)$ is defined as the negative derivative of the output at the switching instant divided by the frequency. The superscript $^{-}$ implies a very short time shift before the switching. This is important for systems in which the output or its derivative change instantaneously by the hysteresis switching. The tilde indicates the periodicity of the signal. For more complex self-oscillations a set of Tsypkin's loci must be defined, like for asymmetrical oscillations one for the switching in between the period and one for the end of the period.

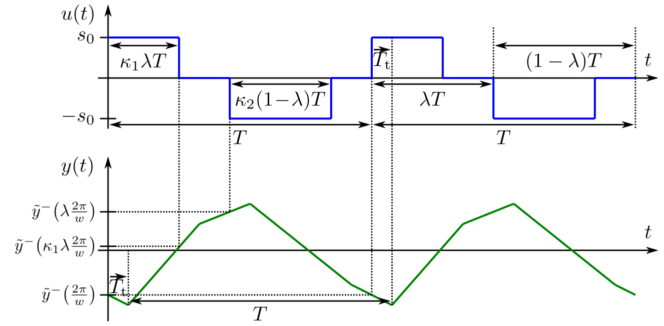

Fig. 5. General asymmetrical self-oscillation of Type I

3.1 Self-Oscillations of Type I

First, the self-oscillations of Type I are studied. As defined above, the output of the hysteresis passes through all three levels. Without losing generality, the time $t = 0$ is defined as the point in time when the output of the hysteresis is switching to the positive stage. In a general case, the self-oscillation of Type I can be asymmetrical. Fig. 5 shows the output of the hysteresis and the oscillating control loop output for this general case. So, the switching conditions are consequently defined by the control deviations and its derivative at the switching events.

$$\begin{aligned} e\,(0) = e\left(\frac{2\pi}{\omega}\right) &= \delta_2 & \dot{e}\,(0) = \dot{e}\left(\frac{2\pi}{\omega}\right) &> 0 \\ e\left(\kappa_1\lambda\frac{2\pi}{\omega}\right) &= -\delta_1 & \dot{e}\left(\kappa_1\lambda\frac{2\pi}{\omega}\right) &< 0 \\ e\left(\lambda\frac{2\pi}{\omega}\right) &= -\delta_2 & \dot{e}\left(\lambda\frac{2\pi}{\omega}\right) &< 0 \\ e\left((\lambda+\kappa_2-\kappa_2\lambda)\frac{2\pi}{\omega}\right) &= \delta_1 & \dot{e}\left((\lambda+\kappa_2-\kappa_2\lambda)\frac{2\pi}{\omega}\right) &> 0 \end{aligned} \tag{3}$$

But, these asymmetrical self-oscillations are undesirable in practical power electronic applications, because they execute more switching events than necessary leading to higher switching losses and further to a higher ripple on the current. In order to avoid these asymmetrical self-oscillations, a criterion is derived from symmetrical self-oscillations of Type I, which are considered further now. For symmetrical self-oscillation of Type I the following conditions must hold.

$$\kappa_1 = \kappa_2 = \kappa \qquad \lambda = (1-\lambda) = 0.5 \tag{4}$$

Caused by the dead-time T_t, there are in general six different cases to be distinguished. These cases result from the relative shift of the control signal in relation to the time period T and the effective turn-on time κ shown in Fig. 6. It shows the hysteresis output u and the delayed one u' for these six cases.

For all these different cases, the system response to the control signal can be calculated. More precisely, the output value at the switching events have to be evaluated to construct Tsypkin's loci. The exact derivation is quite lengthy and is not shown in this paper. The basic approach for a two-level hysteresis is shown in Åström (1995) and Boiko (2009) and can be applied to three-level hysteresis.

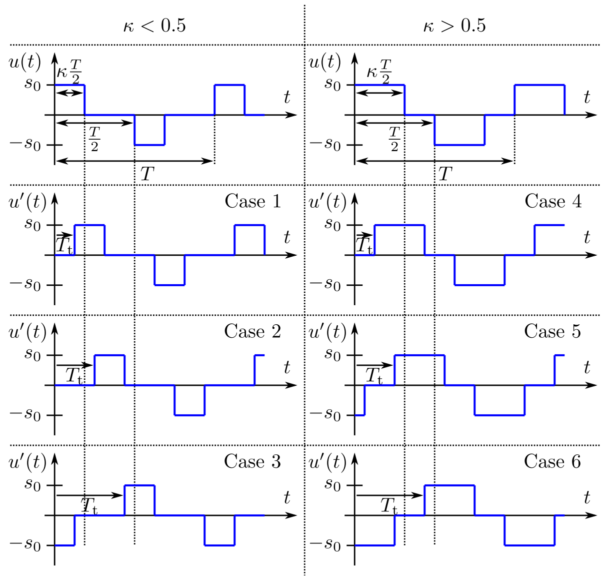

Fig. 6. Different cases of the dead-time T_t dependent shift in relation to κ and the time period T in case of symmetric self-oscillations of Type I

As a result, Tsypkin's loci $\mathcal{J}_\kappa(\omega,\kappa)$ for the switching event at $t = \kappa T/2$ and $\mathcal{J}_{\frac{1}{2}}(\omega,\kappa)$ for the switching event at $t = T/2$ are given. Assuming that the matrix $(\boldsymbol{I}+\mathrm{e}^{\boldsymbol{A}\frac{2\pi}{\omega}})$ is invertible for all ω (equivalent to $\boldsymbol{A}$ having no eigenvalues on the imaginary axis), Tsypkin's loci can be given as follows. Some of the different cases leading to the same result. For $\mathcal{J}_\kappa(\omega,\kappa)$, the cases 1, 4, 5 are equal as well as the cases 2, 3, 6.

$$\begin{aligned} \mathcal{J}_\kappa(\omega,\kappa) = (-1)^l \Bigg\{ &\frac{1}{\omega} s_0 \boldsymbol{c}^{\mathrm{T}} \Bigg[\left(\boldsymbol{I}+\mathrm{e}^{\boldsymbol{A}\frac{\pi}{\omega}}\right)^{-1} \\ &\left(\boldsymbol{I}+\mathrm{e}^{\boldsymbol{A}\frac{\pi}{\omega}} - \mathrm{e}^{\boldsymbol{A}\left(\frac{(l+1)\pi}{\omega}-T_t\right)} - \mathrm{e}^{\boldsymbol{A}\left(\frac{(l+\kappa)\pi}{\omega}-T_t\right)}\right) - \boldsymbol{I}\Bigg]\boldsymbol{b} \\ &+ \mathrm{j}s_0 \Bigg[\boldsymbol{c}^{\mathrm{T}}\left(\boldsymbol{I}+\mathrm{e}^{\boldsymbol{A}\frac{\pi}{\omega}}\right)^{-1}\boldsymbol{A}^{-1} \\ &\left(\boldsymbol{I}+\mathrm{e}^{\boldsymbol{A}\frac{\pi}{\omega}} - \mathrm{e}^{\boldsymbol{A}\left(\frac{(l+1)\pi}{\omega}-T_t\right)} - \mathrm{e}^{\boldsymbol{A}\left(\frac{(l+\kappa)\pi}{\omega}-T_t\right)}\right)\boldsymbol{b} - d\Bigg]\Bigg\} \\ &\text{for } l\frac{\pi}{T_t} < \omega < (l+\kappa)\frac{\pi}{T_t} \end{aligned} \tag{5}$$

$$\begin{aligned} \mathcal{J}_\kappa(\omega,\kappa) = (-1)^l \Bigg\{ &\frac{1}{\omega} s_0 \boldsymbol{c}^{\mathrm{T}} \Bigg[\left(\boldsymbol{I}+\mathrm{e}^{\boldsymbol{A}\frac{\pi}{\omega}}\right)^{-1} \\ &\left(-\mathrm{e}^{\boldsymbol{A}\left(\frac{(l+1)\pi}{\omega}-T_t\right)} + \mathrm{e}^{\boldsymbol{A}\left(\frac{(l+1+\kappa)\pi}{\omega}-T_t\right)}\right)\Bigg]\boldsymbol{b} \\ &+ \mathrm{j}s_0 \Bigg[\boldsymbol{c}^{\mathrm{T}}\left(\boldsymbol{I}+\mathrm{e}^{\boldsymbol{A}\frac{\pi}{\omega}}\right)^{-1}\boldsymbol{A}^{-1} \\ &\left(-\mathrm{e}^{\boldsymbol{A}\left(\frac{(l+1)\pi}{\omega}-T_t\right)} + \mathrm{e}^{\boldsymbol{A}\left(\frac{(l+1+\kappa)\pi}{\omega}-T_t\right)}\right)\boldsymbol{b}\Bigg]\Bigg\} \\ &\text{for } (l+\kappa)\frac{\pi}{T_t} < \omega < (l+1)\frac{\pi}{T_t} \end{aligned} \tag{6}$$

For $\mathcal{J}_{\frac{1}{2}}(\omega,\kappa)$, the cases 1, 2, 4 are equal as well as the cases 3, 5, 6.

$$\mathcal{J}_{\frac{1}{2}}(\omega,\kappa) = (-1)^l \Bigg\{ \frac{1}{\omega} s_0 \boldsymbol{c}^{\mathrm{T}} \Bigg[\left(\boldsymbol{I} + \mathrm{e}^{\boldsymbol{A}\frac{\pi}{\omega}}\right)^{-1} \left(-\mathrm{e}^{\boldsymbol{A}\left(\frac{(l+1)\pi}{\omega} - T_{\mathrm{t}}\right)} + \mathrm{e}^{\boldsymbol{A}\left(\frac{(l+1-\kappa)\pi}{\omega} - T_{\mathrm{t}}\right)} \right) \Bigg] \boldsymbol{b} + \mathrm{j} s_0 \Bigg[\boldsymbol{c}^{\mathrm{T}} \left(\boldsymbol{I} + \mathrm{e}^{\boldsymbol{A}\frac{\pi}{\omega}}\right)^{-1} \boldsymbol{A}^{-1} \left(-\mathrm{e}^{\boldsymbol{A}\left(\frac{(l+1)\pi}{\omega} - T_{\mathrm{t}}\right)} + \mathrm{e}^{\boldsymbol{A}\left(\frac{(l+1-\kappa)\pi}{\omega} - T_{\mathrm{t}}\right)} \right) \boldsymbol{b} \Bigg] \Bigg\} \quad \text{for } l\frac{\pi}{T_{\mathrm{t}}} < \omega < (l+1-\kappa)\frac{\pi}{T_{\mathrm{t}}} \tag{7}$$

$$\mathcal{J}_{\frac{1}{2}}(\omega,\kappa) = (-1)^l \Bigg\{ \frac{1}{\omega} s_0 \boldsymbol{c}^{\mathrm{T}} \Bigg[\left(\boldsymbol{I} + \mathrm{e}^{\boldsymbol{A}\frac{\pi}{\omega}}\right)^{-1} \left(\boldsymbol{I} + \mathrm{e}^{\boldsymbol{A}\frac{\pi}{\omega}} - \mathrm{e}^{\boldsymbol{A}\left(\frac{(l+1)\pi}{\omega} - T_{\mathrm{t}}\right)} - \mathrm{e}^{\boldsymbol{A}\left(\frac{(l+2-\kappa)\pi}{\omega} - T_{\mathrm{t}}\right)} \right) - \boldsymbol{I} \Bigg] \boldsymbol{b} + \mathrm{j} s_0 \Bigg[\boldsymbol{c}^{\mathrm{T}} \left(\boldsymbol{I} + \mathrm{e}^{\boldsymbol{A}\frac{\pi}{\omega}}\right)^{-1} \boldsymbol{A}^{-1} \left(\boldsymbol{I} + \mathrm{e}^{\boldsymbol{A}\frac{\pi}{\omega}} - \mathrm{e}^{\boldsymbol{A}\left(\frac{(l+1)\pi}{\omega} - T_{\mathrm{t}}\right)} - \mathrm{e}^{\boldsymbol{A}\left(\frac{(l+2-\kappa)\pi}{\omega} - T_{\mathrm{t}}\right)} \right) \boldsymbol{b} - d \Bigg] \Bigg\} \quad \text{for } (l+1-\kappa)\frac{\pi}{T_{\mathrm{t}}} < \omega < (l+1)\frac{\pi}{T_{\mathrm{t}}} \tag{8}$$

Now, the conditions for a symmetrical self-oscillation of Type I in terms of Tsypkin's loci result in

$$\begin{array}{ll} \operatorname{Im} \mathcal{J}_{\kappa}(\omega,\kappa) = -\delta_1 & \operatorname{Re} \mathcal{J}_{\kappa}(\omega,\kappa) < 0 \\ \operatorname{Im} \mathcal{J}_{\frac{1}{2}}(\omega,\kappa) = -\delta_2 & \operatorname{Re} \mathcal{J}_{\frac{1}{2}}(\omega,\kappa) < 0 \end{array} \tag{9}$$

In general for asymmetrical self-oscillations of Type I, a set of four Tsypkin's loci must be defined with the four parameters ω, λ, κ_1 and κ_2.

To analyze the local stability of the self-oscillations which satisfy the conditions of (9), a small initial perturbation $\boldsymbol{x}_{\delta 0}$ at $t = 0$ from the periodical solution of the state variables $\tilde{\boldsymbol{x}}(0)$ is investigated.

$$\boldsymbol{x}(0) = \tilde{\boldsymbol{x}}(0) + \boldsymbol{x}_{\delta 0} \tag{10}$$

Now the propagation of the initial perturbation over half of a switching cycle can be studied. Caused by the distortion, the points in time of the switching events will change. So the states at $t = \kappa\frac{T}{2} + t_{\delta 1}$ and $t = \frac{T}{2} + t_{\delta 2}$ becomes

$$\boldsymbol{x}\left(\kappa\frac{T}{2} + t_{\delta 1}\right) \approx \tilde{\boldsymbol{x}}\left(\kappa\frac{T}{2}\right) + \boldsymbol{W}_{\kappa} \cdot \boldsymbol{x}_{\delta 0} \tag{11}$$

$$\boldsymbol{x}\left(\frac{T}{2} + t_{\delta 2}\right) \approx \tilde{\boldsymbol{x}}\left(\frac{T}{2}\right) + \boldsymbol{W}_{\frac{1}{2}} \cdot \boldsymbol{x}_{\delta 1} \tag{12}$$

$$\approx \tilde{\boldsymbol{x}}\left(\frac{T}{2}\right) + \boldsymbol{W}_{\frac{1}{2}} \cdot \boldsymbol{W}_{\kappa} \cdot \boldsymbol{x}_{\delta 0} \tag{13}$$

where

$$\boldsymbol{W}_{\kappa} = \left(\boldsymbol{I} - \frac{\dot{\tilde{\boldsymbol{x}}}^{-}\left(\kappa\frac{T}{2}\right) \cdot \boldsymbol{c}^{\mathrm{T}}}{\boldsymbol{c}^{\mathrm{T}} \cdot \dot{\tilde{\boldsymbol{x}}}^{-}\left(\kappa\frac{T}{2}\right)} \right) \cdot \mathrm{e}^{\boldsymbol{A}\kappa\lambda\frac{T}{2}} \tag{14}$$

$$\boldsymbol{W}_{\frac{1}{2}} = \left(\boldsymbol{I} - \frac{\dot{\tilde{\boldsymbol{x}}}^{-}\left(\frac{T}{2}\right) \cdot \boldsymbol{c}^{\mathrm{T}}}{\boldsymbol{c}^{\mathrm{T}} \cdot \dot{\tilde{\boldsymbol{x}}}^{-}\left(\frac{T}{2}\right)} \right) \cdot \mathrm{e}^{\boldsymbol{A}(1-\kappa)\lambda\frac{T}{2}} \tag{15}$$

So, the self-oscillation is locally asymptotically stable if and only if the perturbation decreases over time. Analytically, this means if and only if the largest absolute value of the eigenvalues of the product of $\boldsymbol{W}_{\kappa}$ and $\boldsymbol{W}_{\frac{1}{2}}$ is smaller than one.

$$\rho\left(\boldsymbol{W}_{\kappa} \cdot \boldsymbol{W}_{\frac{1}{2}}\right) < 1 \tag{16}$$

Caused by higher switching losses in the power electronic, this self-oscillations of Type I are undesirable and should be avoided. So the aim is to enlarge the time of the zero level of the hysteresis, because during this time only the self-reinforcing tendencies of the system decrease the state values. So, the hysteresis limit δ_2 must set higher to increase the relative time of the zero level defined by $(1-\kappa)$. A criterion can be derived from the condition (9) for a symmetrical limit cycle. So the critical value for the outer hysteresis limit $\delta_{2,\mathrm{crit}}$ for a given inner limit δ_1 leading to a critical κ_{crit} and can be evaluate by

$$\begin{array}{ll} \operatorname{Im} \mathcal{J}_{\kappa}(\omega,\kappa_{\mathrm{crit}}) = -\delta_1 & \operatorname{Re} \mathcal{J}_{\kappa}(\omega,\kappa_{\mathrm{crit}}) < 0 \\ \operatorname{Im} \mathcal{J}_{\frac{1}{2}}(\omega,\kappa_{\mathrm{crit}}) = -\delta_{2,\mathrm{crit}} & \operatorname{Re} \mathcal{J}_{\frac{1}{2}}(\omega,\kappa_{\mathrm{crit}}) = 0 \end{array} \tag{17}$$

Graphically, this means that the output value touches the hysteresis limit at the point $t = \frac{T}{2}$. So, there is no intersection of the limit and consequently no switching. It can be shown that if there is no symmetrical self-oscillation then there is also no asymmetrical one. This critical hysteresis limit $\delta_{2,\mathrm{crit}}$ is the theoretical limitation of the existence of the Type I oscillation. Nevertheless, it is possible that this self-oscillation even not occurs with smaller hysteresis limits δ_2, because the area of attractivity becomes smaller the larger this limit is.

3.2 Self-Oscillations of Type II and Type III

The self-oscillations of Type II and Type III can be analyzed together. The only difference between these two is the output value of the hysteresis. But generalizing the values to s_+ and s_- for a higher and lower level, the two types can be described by one set of equations. Consequently, the levels for Type II are $s_+ = s_0$ and $s_- = 0$, for Type III $s_+ = 0$ and $s_- = -s_0$. A positive set point r leads to Type II and a negative one to Type III.

The switching conditions for both types are

$$\begin{array}{ll} e\,(0) = e\left(\dfrac{2\pi}{\omega}\right) = \delta_1 & \dot{e}\,(0) = \dot{e}\left(\dfrac{2\pi}{\omega}\right) > 0 \\ e\left(\lambda\dfrac{2\pi}{\omega}\right) = -\delta_1 & \dot{e}\left(\lambda\dfrac{2\pi}{\omega}\right) < 0 \end{array} \tag{18}$$

As for symmetrical self-oscillations of Type I, there are also six different cases for the relative shift of control signal in relation to the period duration time T and the duty cycle λ shown in Fig. 7.

Some cases lead to the same result of the Tsypkin's loci description. Assuming that the matrix $(\boldsymbol{I} - \mathrm{e}^{\boldsymbol{A}\frac{2\pi}{\omega}})$ is invertible for all ω, the equations can be given as follows. For $\mathcal{J}_{\lambda}(\omega,\lambda)$, the cases 1, 4, 5 are equal as well as the cases 2, 3, 6.

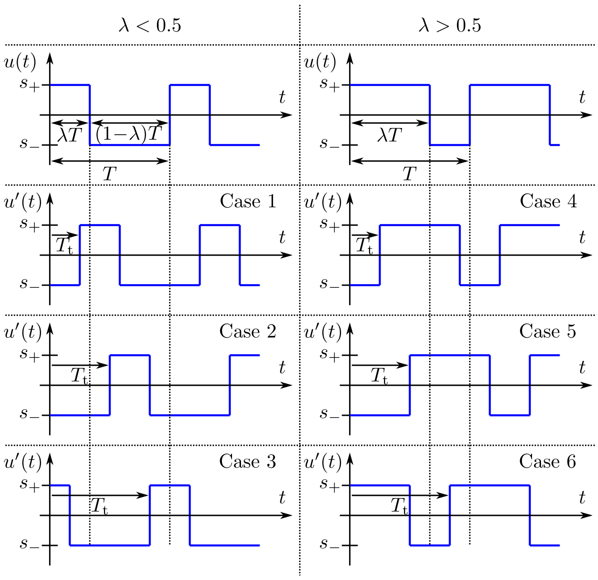

Fig. 7. Different cases of the dead-time T_t dependent shift in relation to the duty cycle λ and the time period T in case of asymmetric self-oscillations of Type II or Type III

$$\begin{aligned}\mathcal{J}_\lambda(\omega,\lambda) = \frac{1}{\omega}\boldsymbol{c}^\mathrm{T}\Bigg[&\left(\boldsymbol{I}-\mathrm{e}^{\boldsymbol{A}\frac{2\pi}{\omega}}\right)^{-1}\\ &\Bigg(\left(\boldsymbol{I}-\mathrm{e}^{\boldsymbol{A}\frac{2\pi}{\omega}}+\mathrm{e}^{\boldsymbol{A}\left(\frac{(l+1)2\pi}{\omega}-T_\mathrm{t}\right)}-\mathrm{e}^{\boldsymbol{A}\left(\frac{(l+\lambda)2\pi}{\omega}-T_\mathrm{t}\right)}\right)s_+\\ &+\left(-\mathrm{e}^{\boldsymbol{A}\left(\frac{(l+1)2\pi}{\omega}-T_\mathrm{t}\right)}+\mathrm{e}^{\boldsymbol{A}\left(\frac{(l+\lambda)2\pi}{\omega}-T_\mathrm{t}\right)}\right)s_-\Bigg)-\boldsymbol{I}s_+\Bigg]\boldsymbol{b}\\ &+\mathrm{j}\Bigg[\boldsymbol{c}^\mathrm{T}\left(\boldsymbol{I}-\mathrm{e}^{\boldsymbol{A}\frac{2\pi}{\omega}}\right)^{-1}\boldsymbol{A}^{-1}\\ &\Bigg(\left(\boldsymbol{I}-\mathrm{e}^{\boldsymbol{A}\frac{2\pi}{\omega}}+\mathrm{e}^{\boldsymbol{A}\left(\frac{(l+1)2\pi}{\omega}-T_\mathrm{t}\right)}-\mathrm{e}^{\boldsymbol{A}\left(\frac{(l+\lambda)2\pi}{\omega}-T_\mathrm{t}\right)}\right)s_+\\ &+\left(-\mathrm{e}^{\boldsymbol{A}\left(\frac{(l+1)2\pi}{\omega}-T_\mathrm{t}\right)}+\mathrm{e}^{\boldsymbol{A}\left(\frac{(l+\lambda)2\pi}{\omega}-T_\mathrm{t}\right)}\right)s_-\Bigg)\boldsymbol{b}-ds_+\Bigg]\\ &\text{for } l\frac{2\pi}{T_\mathrm{t}}<\omega<(l+\lambda)\frac{2\pi}{T_\mathrm{t}}\end{aligned}\tag{19}$$

$$\begin{aligned}\mathcal{J}_\lambda(\omega,\lambda) = \frac{1}{\omega}\boldsymbol{c}^\mathrm{T}\Bigg[&\left(\boldsymbol{I}-\mathrm{e}^{\boldsymbol{A}\frac{2\pi}{\omega}}\right)^{-1}\\ &\Bigg(\left(\boldsymbol{I}-\mathrm{e}^{\boldsymbol{A}\frac{2\pi}{\omega}}-\mathrm{e}^{\boldsymbol{A}\left(\frac{(l+1)2\pi}{\omega}-T_\mathrm{t}\right)}+\mathrm{e}^{\boldsymbol{A}\left(\frac{(l+1+\lambda)2\pi}{\omega}-T_\mathrm{t}\right)}\right)s_-\\ &+\left(\mathrm{e}^{\boldsymbol{A}\left(\frac{(l+1)2\pi}{\omega}-T_\mathrm{t}\right)}-\mathrm{e}^{\boldsymbol{A}\left(\frac{(l+1+\lambda)2\pi}{\omega}-T_\mathrm{t}\right)}\right)s_+\Bigg)-\boldsymbol{I}s_-\Bigg]\boldsymbol{b}\\ &+\mathrm{j}\Bigg[\boldsymbol{c}^\mathrm{T}\left(\boldsymbol{I}-\mathrm{e}^{\boldsymbol{A}\frac{2\pi}{\omega}}\right)^{-1}\boldsymbol{A}^{-1}\\ &\Bigg(\left(\boldsymbol{I}-\mathrm{e}^{\boldsymbol{A}\frac{2\pi}{\omega}}-\mathrm{e}^{\boldsymbol{A}\left(\frac{(l+1)2\pi}{\omega}-T_\mathrm{t}\right)}+\mathrm{e}^{\boldsymbol{A}\left(\frac{(l+1+\lambda)2\pi}{\omega}-T_\mathrm{t}\right)}\right)s_-\\ &+\left(\mathrm{e}^{\boldsymbol{A}\left(\frac{(l+1)2\pi}{\omega}-T_\mathrm{t}\right)}-\mathrm{e}^{\boldsymbol{A}\left(\frac{(l+1+\lambda)2\pi}{\omega}-T_\mathrm{t}\right)}\right)s_+\Bigg)\boldsymbol{b}-ds_-\Bigg]\\ &\text{for } (l+\lambda)\frac{2\pi}{T_\mathrm{t}}<\omega<(l+1)\frac{2\pi}{T_\mathrm{t}}\end{aligned}\tag{20}$$

For $\mathcal{J}_1(\omega,\lambda)$, the cases 1, 2, 4 are equal as well as the cases 3, 5, 6.

$$\begin{aligned}\mathcal{J}_1(\omega,\lambda) = \frac{1}{\omega}\boldsymbol{c}^\mathrm{T}\Bigg[&\left(\boldsymbol{I}-\mathrm{e}^{\boldsymbol{A}\frac{2\pi}{\omega}}\right)^{-1}\\ &\Bigg(\left(\boldsymbol{I}-\mathrm{e}^{\boldsymbol{A}\frac{2\pi}{\omega}}+\mathrm{e}^{\boldsymbol{A}\left(\frac{(l+1)2\pi}{\omega}-T_\mathrm{t}\right)}-\mathrm{e}^{\boldsymbol{A}\left(\frac{(l+1-\lambda)2\pi}{\omega}-T_\mathrm{t}\right)}\right)s_-\\ &+\left(-\mathrm{e}^{\boldsymbol{A}\left(\frac{(l+1)2\pi}{\omega}-T_\mathrm{t}\right)}+\mathrm{e}^{\boldsymbol{A}\left(\frac{(l+1+\lambda)2\pi}{\omega}-T_\mathrm{t}\right)}\right)s_+\Bigg)-\boldsymbol{I}s_-\Bigg]\boldsymbol{b}\\ &+\mathrm{j}\Bigg[\boldsymbol{c}^\mathrm{T}\left(\boldsymbol{I}-\mathrm{e}^{\boldsymbol{A}\frac{2\pi}{\omega}}\right)^{-1}\boldsymbol{A}^{-1}\\ &\Bigg(\left(\boldsymbol{I}-\mathrm{e}^{\boldsymbol{A}\frac{2\pi}{\omega}}+\mathrm{e}^{\boldsymbol{A}\left(\frac{(l+1)2\pi}{\omega}-T_\mathrm{t}\right)}-\mathrm{e}^{\boldsymbol{A}\left(\frac{(l+1+\lambda)2\pi}{\omega}-T_\mathrm{t}\right)}\right)s_-\\ &+\left(-\mathrm{e}^{\boldsymbol{A}\left(\frac{(l+1)2\pi}{\omega}-T_\mathrm{t}\right)}+\mathrm{e}^{\boldsymbol{A}\left(\frac{(l+1+\lambda)2\pi}{\omega}-T_\mathrm{t}\right)}\right)s_+\Bigg)\boldsymbol{b}-ds_-\Bigg]\\ &\text{for } l\frac{2\pi}{T_\mathrm{t}}<\omega<(l+1-\lambda)\frac{2\pi}{T_\mathrm{t}}\end{aligned}\tag{21}$$

$$\begin{aligned}\mathcal{J}_1(\omega,\lambda) = \frac{1}{\omega}\boldsymbol{c}^\mathrm{T}\Bigg[&\left(\boldsymbol{I}-\mathrm{e}^{\boldsymbol{A}\frac{2\pi}{\omega}}\right)^{-1}\\ &\Bigg(\left(\boldsymbol{I}-\mathrm{e}^{\boldsymbol{A}\frac{2\pi}{\omega}}-\mathrm{e}^{\boldsymbol{A}\left(\frac{(l+1)2\pi}{\omega}-T_\mathrm{t}\right)}+\mathrm{e}^{\boldsymbol{A}\left(\frac{(l+2-\lambda)2\pi}{\omega}-T_\mathrm{t}\right)}\right)s_+\\ &+\left(\mathrm{e}^{\boldsymbol{A}\left(\frac{(l+1)2\pi}{\omega}-T_\mathrm{t}\right)}-\mathrm{e}^{\boldsymbol{A}\left(\frac{(l+2-\lambda)2\pi}{\omega}-T_\mathrm{t}\right)}\right)s_-\Bigg)-\boldsymbol{I}s_+\Bigg]\boldsymbol{b}\\ &+\mathrm{j}\Bigg[\boldsymbol{c}^\mathrm{T}\left(\boldsymbol{I}-\mathrm{e}^{\boldsymbol{A}\frac{2\pi}{\omega}}\right)^{-1}\boldsymbol{A}^{-1}\\ &\Bigg(\left(\boldsymbol{I}-\mathrm{e}^{\boldsymbol{A}\frac{2\pi}{\omega}}-\mathrm{e}^{\boldsymbol{A}\left(\frac{(l+1)2\pi}{\omega}-T_\mathrm{t}\right)}+\mathrm{e}^{\boldsymbol{A}\left(\frac{(l+2-\lambda)2\pi}{\omega}-T_\mathrm{t}\right)}\right)s_+\\ &+\left(\mathrm{e}^{\boldsymbol{A}\left(\frac{(l+1)2\pi}{\omega}-T_\mathrm{t}\right)}-\mathrm{e}^{\boldsymbol{A}\left(\frac{(l+2-\lambda)2\pi}{\omega}-T_\mathrm{t}\right)}\right)s_-\Bigg)\boldsymbol{b}-ds_+\Bigg]\\ &\text{for } (l+1-\lambda)\frac{2\pi}{T_\mathrm{t}}<\omega<(l+1)\frac{2\pi}{T_\mathrm{t}}\end{aligned}\tag{22}$$

The conditions for an asymmetrical self-oscillation of Type II or Type III in terms of Tsypkin's loci result in

$$\begin{aligned}\operatorname{Im}\mathcal{J}_\lambda(\omega,\lambda) &= -r-\delta_1 \qquad \operatorname{Re}\mathcal{J}_\lambda(\omega,\lambda)<0\\ \operatorname{Im}\mathcal{J}_1(\omega,\lambda) &= -r+\delta_1 \qquad \operatorname{Re}\mathcal{J}_1(\omega,\lambda)>0\end{aligned}\tag{23}$$

The local stability of the self-oscillation can also be analyzed by the concept of a small initial perturbation and its propagation over time. The whole period is considered. So the states at $t=\lambda T+t_{\delta 1}$ and $t=T+t_{\delta 2}$ becomes

$$\boldsymbol{x}\left(\lambda T+t_{\delta 1}\right)\approx\tilde{\boldsymbol{x}}\left(\lambda T\right)+\boldsymbol{W}_\lambda\cdot\boldsymbol{x}_{\delta 0}\tag{24}$$
$$\boldsymbol{x}\left(T+t_{\delta 2}\right)\approx\tilde{\boldsymbol{x}}\left(T\right)+\boldsymbol{W}_1\cdot\boldsymbol{x}_{\delta 1}\tag{25}$$
$$\approx\tilde{\boldsymbol{x}}\left(T\right)+\boldsymbol{W}_1\cdot\boldsymbol{W}_\lambda\cdot\boldsymbol{x}_{\delta 0}\tag{26}$$

where

$$\boldsymbol{W}_\lambda=\left(\boldsymbol{I}-\frac{\dot{\tilde{\boldsymbol{x}}}^-(\lambda T)\cdot\boldsymbol{c}^\mathrm{T}}{\boldsymbol{c}^\mathrm{T}\cdot\dot{\tilde{\boldsymbol{x}}}^-(\lambda T)}\right)\cdot\mathrm{e}^{\boldsymbol{A}\lambda T}\tag{27}$$

$$\boldsymbol{W}_1=\left(\boldsymbol{I}-\frac{\dot{\tilde{\boldsymbol{x}}}^-(T)\cdot\boldsymbol{c}^\mathrm{T}}{\boldsymbol{c}^\mathrm{T}\cdot\dot{\tilde{\boldsymbol{x}}}^-(T)}\right)\cdot\mathrm{e}^{\boldsymbol{A}(1-\lambda)T}\tag{28}$$

So, the self-oscillation is locally asymptotically stable if and only if

$$\rho\left(\boldsymbol{W}_\lambda\cdot\boldsymbol{W}_1\right)<1\tag{29}$$

4. APPLICATION TO DIRECT-CURRENT CONTROL

Using the Tsypkin's loci, the behavior of the direct-current control loop with a three-level hysteresis controller can be analyzed. For the H-bridge with RL-load (Fig. 1), the state matrices and vectors become scalars.

$$\boldsymbol{A} = -\frac{R}{L}, \quad \boldsymbol{b} = \frac{1}{L}, \quad \boldsymbol{c}^{\mathrm{T}} = 1, \quad d = 0 \tag{30}$$

In the following, only positive set points are considered leading to Type II oscillations ($s_- = 0$, $s_+ = U_{\mathrm{dc}}$). The outer hysteresis limit δ_2 is set as big enough in order to avoid Type I oscillations. Furthermore, restricting to the cases 1 and 4, Tsypkin's loci for the H-bridge with RL-load result in

$$\begin{aligned}\mathcal{J}_\lambda(\omega, \lambda) = {} & \frac{U_{\mathrm{dc}}}{\omega L} \cdot \frac{\mathrm{e}^{-\frac{R}{L}\left(\frac{2\pi}{\omega} - T_{\mathrm{t}}\right)} - \mathrm{e}^{-\frac{R}{L}\left(\frac{\lambda 2\pi}{\omega} - T_{\mathrm{t}}\right)}}{1 - \mathrm{e}^{-\frac{R}{L}\frac{2\pi}{\omega}}} \\ & - \mathrm{j}\frac{U_{\mathrm{dc}}}{R} \cdot \left(1 + \frac{\mathrm{e}^{-\frac{R}{L}\left(\frac{2\pi}{\omega} - T_{\mathrm{t}}\right)} - \mathrm{e}^{-\frac{R}{L}\left(\frac{\lambda 2\pi}{\omega} - T_{\mathrm{t}}\right)}}{1 - \mathrm{e}^{-\frac{R}{L}\frac{2\pi}{\omega}}}\right)\end{aligned} \tag{31}$$

$$\begin{aligned}\mathcal{J}_1(\omega, \lambda) = {} & -\frac{U_{\mathrm{dc}}}{\omega L} \cdot \frac{\mathrm{e}^{-\frac{R}{L}\left(\frac{2\pi}{\omega} - T_{\mathrm{t}}\right)} - \mathrm{e}^{-\frac{R}{L}\left(\frac{(1+\lambda) 2\pi}{\omega} - T_{\mathrm{t}}\right)}}{1 - \mathrm{e}^{-\frac{R}{L}\frac{2\pi}{\omega}}} \\ & + \mathrm{j}\frac{U_{\mathrm{dc}}}{R} \cdot \frac{\mathrm{e}^{-\frac{R}{L}\left(\frac{2\pi}{\omega} - T_{\mathrm{t}}\right)} - \mathrm{e}^{-\frac{R}{L}\left(\frac{(1+\lambda) 2\pi}{\omega} - T_{\mathrm{t}}\right)}}{1 - \mathrm{e}^{-\frac{R}{L}\frac{2\pi}{\omega}}}\end{aligned} \tag{32}$$

With these expressions for Tsypkin's loci, equation (23) can be solved for the switching frequency ω and the duty cycle λ with different values of the set point r and the hysteresis limit δ_1. In general, an analytical solution is not possible. So, the set of equations is solved numerically. (The solutions hold also the restriction to case 1 or 4.) Fig. 8 shows the result of this analysis.

The parameters are set to: $R = 1.5\,\Omega$, $L = 0.3\,\mathrm{mH}$, $T_{\mathrm{t}} = 0.1\,\mathrm{ms}$, $U_{\mathrm{dc}} = 12\,\mathrm{V}$.

For all different values of the hysteresis limit δ_1, the duty cycle is equal to 0.5 for the set point $r = 4$. For other set points, the calculated duty cycles differ for the different hysteresis limits as well as from the "ideal" duty cycle for which the control deviation would be zero (dashed line in Fig. 8). The difference increases with the difference between the set point and this middle point $r = 4$. A smaller hysteresis limit leads to a higher the switching frequency of the power electronics and vice versa. At the duty cycle $\lambda = 0.5$, the frequency is the highest and decreases to both sides of this value symmetrically. Knowing the duty cycle λ of the self-oscillation, it is also possible to calculate the mean output value of the control loop.

$$\overline{y} = [s_+ \cdot \lambda + s_- \cdot (1 - \lambda)] \cdot G(0) \tag{33}$$

5. CONCLUSION

In this paper, Tsypkin's method is applied to analyze the switching behavior of three-level hysteresis controllers used for direct current control in H-bridge based applications. There are three different types of self-oscillations in such control loops possible. For these types, Tsypkin's loci were given. So, the behavior of direct current could be analyzed.

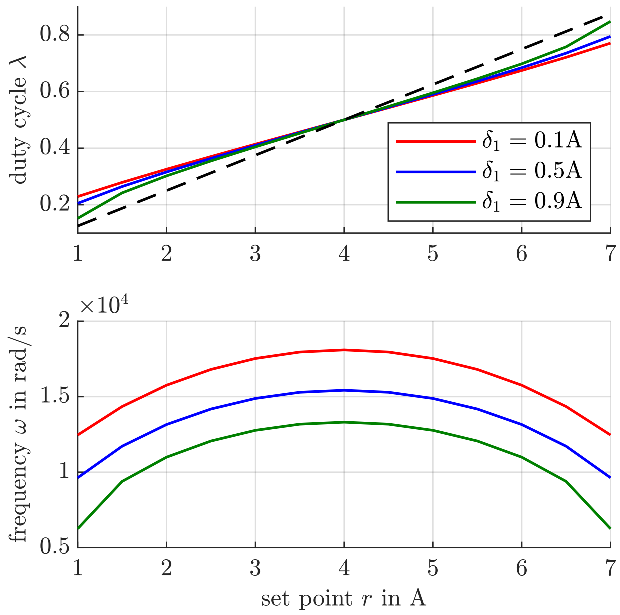

Fig. 8. Duty cycle and switching frequency of the power electronic in the direct-current control loop for different values of hysteresis limit δ_1

REFERENCES

Åström, K.J. (1995). Oscillations in systems with relay feedback. In K.J. Åström et al. (ed.), *Adaptive Control, Filtering, and Signal Processing*, volume 74 of *The IMA Volumes in Mathematics and its Applications*, 1–25. Springer, New York.

Atherton, D.P. (1982). *Nonlinear Control Engineering: Describing Function, Analysis and Design.* van Nostrand Reinhold, New York, student edition.

Boiko, I. (2009). *Discontinuous Control Systems.* Birkhäuser, Boston.

Gatlan, C. and Gatlan, L. (1997). Ac to dc pwm voltage source converter under hysteresis current control. In *ISIE '97 Proceeding of the IEEE International Symposium on Industrial Electronics*, 469–473. New York.

Gelb, A. and Vander Velde, W.E. (1968). *Multiple-Input Describing Functions and Nonlinear System Design.* McGraw-Hill, New York.

Holmes, D.G. and Lipo, T.A. (2003). *Pulse Width Modulation for Power Converters: Principles and Practice.* Wiley-Interscience, IEEE Press, Hoboken, Piscataway.

Johansson, K.H. (1997). *Relay Feedback and Multivariable Control.* Doctoral Dissertation, Lund Institute of Technology.

Mao, H., Yang, X., Chen, Z., and Wang, Z. (2012). A hysteresis current controller for single-phase three-level voltage source inverters. *IEEE Transactions on Power Electronics*, 27(7), 3330–3339.

Tsypkin, Y.Z. (1984). *Relay control systems.* Cambridge UP, Cambridge.

Unbehauen, H. (2009). *Regelungstechnik II.* Vieweg und Teubner, Wiesbaden, 9th edition.